Copy 6

RM E52C17

NACA

RESEARCH MEMORANDUM

EXPERIMENTAL INVESTIGATION OF A CONSERVATIVELY DESIGNED

TURBINE AT FOUR ROTOR-BLADE SOLIDITIES

By Jack A. Heller, Rose L. Whitney, and
Richard H. Cavicchi

Lewis Flight Propulsion Laboratory
Cleveland, Ohio

NATIONAL ADVISORY COMMITTEE
FOR AERONAUTICS

WASHINGTON
July 17, 1952

2497

NATIONAL ADVISORY COMMITTEE FOR AERONAUTICS

RESEARCH MEMORANDUM

EXPERIMENTAL INVESTIGATION OF A CONSERVATIVELY DESIGNED

TURBINE AT FOUR ROTOR-BLADE SOLIDITIES

By Jack A. Heller, Rose L. Whitney, and
Richard H. Cavicchi

SUMMARY

In order to determine limiting values of the aerodynamic parameters used in turbine design, a study of several turbine designs suitable for application in current aircraft power plants is being made. As a first phase in this program, the performance of a single-stage turbine of conservative design was studied for the purpose of establishing a basis for the comparison of turbine performance of less conservative designs. This turbine was investigated at four rotor-blade solidities ranging from 0.85 to 2.27 in order to determine the effect of solidity upon turbine performance.

The variation in solidity was accomplished by changing the number of blades in each rotor and simultaneously orienting the stator blades so as to maintain values of the aerodynamic parameters nearly constant. Rotors having 64, 44, 32, and 24 blades were used. The same 40-blade stator was used with all four rotors.

The 44-blade-rotor turbine yielded the best efficiency over most of the range of investigation. The value of the maximum brake internal efficiency for the 44-blade-rotor turbine was 0.895. The efficiency at the design point was 0.89. Over most of the range of solidities investigated, the curve of maximum brake internal efficiency was relatively flat. A value of solidity of approximately 1.5 was found to be optimum for this turbine; this corresponds to a value of approximately 0.75 for the coefficient of aerodynamic loading. Variation in the value of the coefficient of aerodynamic loading from 0.55 to 1.00 resulted in less than a 0.01 drop from the maximum efficiency obtainable experimentally.

INTRODUCTION

The design of gas turbines for aircraft power plants includes a consideration of certain aerodynamic parameters, such as rotor-inlet relative Mach number, air turning angle, and degree of reaction. The values

of these parameters should be such as to obtain the design efficiency at
the required work output. In the design of conservative turbines, the
values of rotor-inlet relative Mach number and turning angle encountered
are low and the reaction is generally high. This case offers little
difficulty in obtaining good values of efficiency for the required work
output. For less conservative turbines designed for high work output,
high values of rotor-inlet relative Mach number and turning angle are
necessary together with low, or even negative, values of reaction. In
this case, difficulty arises in obtaining good efficiency for the
required work output. It is anticipated that these parameters have
certain limiting values beyond which turbine efficiency falls off rapidly.

An additional parameter to be considered in the design of turbines
is blade spacing or solidity (ratio of axial chord to blade spacing).
The problem of the selection of this parameter arises in the design of
conservative turbines as well as in the design of high-work-output
turbines.

As the number of rotor blades is reduced, the loading of each blade
increases. If the rotor solidity is too greatly reduced, the negative
pressure gradient on the suction surface in the region of the trailing
edge will become sufficiently large so that separation of flow from the
surface will occur and large losses result. If the blades are more
closely spaced than necessary, that is, the rotor has excessively high
solidity, the boundary-layer friction losses will be unnecessarily large
because of the increased flow surface area.

As part of a program to determine limiting values of the parameters
used in the aerodynamic design, the NACA Lewis laboratory is studying
several turbine designs suitable for application in current aircraft
power plants. This report presents the performance of a single-stage
turbine which is conservative in design, having low rotor-inlet relative
Mach numbers, low turning angles, and high reaction at the rotor root
section. The hub-tip radius ratio is 0.60 and the design tangential
velocity at the rotor exit is zero, thus making the design suitable for
the last stage of a multistage aircraft gas turbine. This conservative
turbine design was investigated first in order to establish a basis for
comparing the performances of less conservative designs. An evaluation
can then be made of the effects of higher Mach numbers relative to the
rotating blades, zero or negative reaction, and higher turning on
turbine performance.

2497

In addition, this turbine was investigated at four rotor-blade solidities ranging from 0.85 to 2.27 in order to determine the effect of solidity upon turbine performance. The over-all performance of each rotor configuration with the same stator was determined in a 14-inch cold-air turbine. The experimental results of this solidity investigation were compared with values of optimum solidity calculated by empirical methods presented in references 1 to 3.

SYMBOLS

The following symbols are used in this report:

A   area (sq ft)

a_{cr} critical velocity of sound, $\sqrt{\left(\frac{2\gamma}{\gamma+1}\right) gRT'}$ (ft/sec)

d   diameter (ft)

E   turbine shaft work (Btu/lb)

F   reaction factor, $\dfrac{W_3{}^2 - W_2{}^2}{W_2{}^2}$

g   acceleration due to gravity (ft/sec^2)

h   specific enthalpy (Btu/lb)

O   exit throat opening (ft)

p   absolute pressure (lb/sq ft)

R   gas constant (ft-lb/(lb)($^\circ$R))

r   radius (ft)

s   blade pitch (ft)

T   temperature ($^\circ$R)

U   blade velocity (ft/sec)

V   absolute velocity of gas (ft/sec)

W   relative velocity of gas (ft/sec)

w   weight-flow rate of gas (lb/sec)

α angle of absolute velocity, measured from tangential direction (deg)

β angle of relative velocity, measured from tangential direction (deg)

γ ratio of specific heats

Δ prefix to indicate change

δ pressure reduction ratio, p/p_0

η_{ad} adiabatic efficiency

η_t brake internal efficiency

θ temperature reduction ratio, T/T_0

σ solidity, ratio of axial chord to blade spacing

ψ coefficient of aerodynamic loading

Subscripts:

des   design

h   hub

m   mean radius

max   maximum

s   isentropic

T   tip

u   tangential

x   axial

0   NACA sea-level air

1,2,   measuring stations (fig. 3)
3,4

Superscripts:

'   stagnation state

"   relative stagnation state

TURBINE DESIGN

General Specifications

The following assigned conditions and assumptions were initially specified at the design point of the turbine:

Equivalent weight flow, $\dfrac{w\sqrt{\theta_1}}{\delta_1}$, lb/sec 16.60

Over-all stagnation pressure ratio, $\dfrac{p_1'}{p_3'}$ 1.751

Equivalent mean blade speed, $\dfrac{U_m}{\sqrt{\theta_1}}$, ft/sec 625

Turbine hub-tip ratio, $\dfrac{r_h}{r_T}$ 0.60

Turbine outer diameter, d_T, ft. 1.167

Tangential component of rotor exit velocity, $\left(\dfrac{V_u}{a_{cr}}\right)_3$ 0

   (1) Free vortex flow exists at the exit of both the stator and rotor.

   (2) Simple radial equilibrium exists at the exit of both the stator and rotor.

   (3) The stagnation pressure and stagnation temperature are uniform over the blade height at the inlet and exit of both the stator and rotor.

   (4) Expansion in the turbine is adiabatic.

   (5) The flow at the stator entrance is uniform.

   (6) Turbine adiabatic efficiency is 0.88.

   (7) The stator stagnation pressure ratio, $\dfrac{p_1'}{p_2'}$, is 1.019.

The design equivalent work output $\Delta h'/\theta_1$ for the turbine is 16.14 Btu per pound. The zero tangential component of absolute velocity at the rotor exit, the low hub-tip radius ratio (0.60), and the relatively small turning angles (51.0° at the mean section) are all typical of the last stage of a multistage aircraft turbine.

Solidity Considerations

In order to isolate the effects of varying the rotor-blade solidity of a turbine, it would be necessary to adjust the profile design so as to maintain constant values of the aerodynamic parameters. This could be accomplished by using a single stator and by designing different rotor profiles for each solidity. In the present investigation, a less time-consuming approximation to this method was employed. The same stator and rotor blades were used for all four solidities investigated. In order to maintain values of the aerodynamic parameters as nearly constant as possible, the orientation of the stator blades was changed while that of the rotor blades remained fixed for each of the rotor solidities investigated. The orientation was determined by maintaining a fixed ratio of the stator throat area to the rotor throat area, assuming the throat openings at the mean section to be the average throat openings over the blade height.

The profile design was originally made for a 40-blade stator and a 44-blade rotor. The resulting area ratio of this design was 0.80, and the stator was adjusted to maintain this value for the other configurations.

The use of this method actually results in slightly different design weight flows, work outputs, and velocity diagrams for each of the configurations. In the determination of the velocity diagrams for the 64-, 32-, and 24-blade-rotor configurations, the rotor-exit air angle β_3 and the stator-exit air angle α_2 at the mean sections were assumed equal to $\sin^{-1}\left(\frac{o}{s}\right)$. The design equivalent blade speed, the turbine efficiency, and the rotor-exit tangential component of the velocity at the mean sections were all maintained at the same values used in the 44-blade-rotor design. The resulting design equivalent weight flows, stagnation pressure ratios, and work outputs are listed in the following table:

Number of blades	$\dfrac{w\sqrt{\theta_1}}{\delta_1}$	$\dfrac{p_1{}'}{p_3{}'}$	$\dfrac{\Delta h'}{\theta_1}$
64	15.61	1.79	16.68
32	17.37	1.78	16.51
24	18.30	1.78	16.66

Table I gives the velocity diagram for the 44-blade-rotor design at the hub, mean, and tip sections, together with the mean-section diagrams for the 64-, 32-, and 24-blade-rotor configurations. It can be seen from the table that maintaining a constant ratio of the stator mean throat area to the rotor mean throat area gives only slightly different values of velocity diagram components, turning, and root reaction factor. The differences in the rotor-inlet relative velocities are of negligible effect because of the low relative Mach numbers involved. For the 64-, 32-, and 24-blade-rotor configurations at the hub and tip, values of $\sin^{-1}\left(\frac{o}{s}\right)$ differ by less than 1.5° from values of exit air angle calculated by using the assumption of free vortex flow.

Stator Blade Profiles

The stator blade profile at each of five radial stations was designed by using an involute of a circle faired into a straight line for the suction surface. The pressure surface was calculated from the one-dimensional flow equation for compressible nonviscous fluids so that the mean velocity would increase through the length of the channel.

The stator blade for the 44-blade-rotor configuration was set so that $\sin^{-1}\left(\frac{o}{s}\right)$ was equal to the design air angle. Profiles of the hub, mean, and tip stator-blade sections are presented in figure 1(a) together with a table of coordinates. The angle settings shown in this figure apply to the 44-blade-rotor configuration.

Forty blades were individually mounted in the outer turbine casing in a manner that permitted the stator-exit angle to be varied so as to maintain the constant ratio of stator-to-rotor mean-throat area of 0.80. The blades were 2.80 inches in span and had an axial chord of 1.25 inches.

Rotor Blade Profiles

The method used in the profile design of the rotor blades was similar to that used for the stator blades. The rotor blade was set so that $\sin^{-1}\left(\frac{o}{s}\right)$ was equal to the design air angle. For the 44-blade-rotor design, 6° positive incidence was assigned at the mean section of the rotor. Because the stator-blade-exit angles were varied for the remaining three configurations and the rotor-blade entrance angle was set at a fixed value, the design incidence angles for these other configurations were all different. The angles of incidence at the mean sections of the rotor entrance were +9.5°, +7.8°, and +8.5° for the 64-, 32-, and 24-blade rotors, respectively. The design angles of incidence at the hub, mean, and tip sections of the four configurations are less than the stalling incidence predicted from cascade investigations reported in reference 3, with the exception of the hub section of the 64-blade rotor

where the design angle of incidence of 13.1° is close to the stalling incidence predicted in reference 3. It is probable that application of the two-dimensional cascade data to the three-dimensional flow in a turbine gives conservative results. Therefore, it was considered that no appreciable increase in loss would be caused directly by the rather high incidence angle at the hub of the 64-blade-rotor configuration. Profiles of the hub, mean, and tip rotor-blade sections, which apply to all four configurations, are presented in figure 1(b), together with a table of coordinates.

The blade span was 2.775 inches and the axial chord was 1.25 inches. The radial tip clearance was 0.025 inch; the axial clearance between the trailing edge of the stator and the leading edge of the rotor was 0.50 inch.

APPARATUS AND PROCEDURE

Dry air at a temperature of approximately 80° F and a pressure of about 25 pounds per square inch absolute was first passed through a filter tank to remove any foreign material present and then ducted to the turbine plenum chamber. At the turbine inlet, survey measurements indicated conditions of uniform flow. After passing through the turbine, the air was removed by the laboratory low-pressure exhaust system. The power output of the turbine was absorbed by an electric dynamometer that was cradle mounted for torque measurement. A photograph of the turbine installation with the top half of the casing removed is shown in figure 2.

Instrumentation

A schematic cross section of the turbine installation showing measuring stations is presented in figure 3. Inlet conditions at station 1 were determined by three stagnation pressure probes and three stagnation thermocouples. The static pressure at the rotor exit was measured with 16 wall taps, all located 1 inch downstream of the rotor in a plane perpendicular to the axis of the turbine. Four of these taps were in the outer casing wall and 12 were equally spaced circumferentially on the inner shroud at station 3. The exit stagnation temperature was measured by four stagnation thermocouples located in the 18-inch-diameter exhaust duct at station 4. The stagnation temperature was measured at station 4 rather than at station 3 in order to obtain measurements in a region where no radial variations of stagnation temperature existed. Heat-transfer calculations show a negligible amount of heat transfer between stations 3 and 4.

Torque was measured with a commercial springless dynamometer scale. Air flow was measured with a submerged 11.75-inch-diameter flat-plate orifice installed in a 24-inch duct in conformance with the specifications

in reference 4. Turbine speed was measured by an electric chronometric tachometer.

The same instruments were used throughout the entire investigation and were read with the following accuracy:

Absolute pressure, in. Hg . . . . ±0.02
Temperature, °R . . . . ±0.5
Orifice pressure drop, in. H$_2$0 . . . . ±0.20
Torque, ft-lb . . . . ±0.30
Rotative speed, rpm . . . . ±10

The probable error in reproducing the brake internal efficiency was less than 0.01.

Procedure and Performance Calculations

Over-all performance data were taken at nominal values of stagnation pressure ratio p_1'/p_3' from 1.20 to the maximum obtainable, while the wheel speed was varied from 0.60 to 1.10 of equivalent design speed in 0.05 intervals (7800 to 14,400 rpm based on an inlet temperature of 540° R).

The brake internal efficiency, which is based on expansion between the entrance and exit stagnation pressures, was used to express turbine performance. It is defined as $\eta_t = \dfrac{E}{(h_1' - h_3')_s}$ where E is the measured turbine shaft work. The ideal enthalpy drop $(h_1' - h_3')_s$ was computed from the values of entrance and exit stagnation pressure and entrance stagnation temperature. The exit stagnation pressure was computed by adding to the measured static pressure a dynamic pressure corresponding to the axial component of the exit velocity computed from continuity considerations. In the following equation based on one-dimensional flow equations, all quantities are known except the stagnation pressure p_3':

$$\frac{w\sqrt{T_3'}}{p_3 A_3} = \frac{p_3'}{p_3}\sqrt{\left(\frac{p_3}{p_3'}\right)^{\frac{2}{\gamma}} - \left(\frac{p_3}{p_3'}\right)^{\frac{\gamma+1}{\gamma}}}\sqrt{\left(\frac{2\gamma}{\gamma-1}\right)\left(\frac{g}{R}\right)}$$

The area A_3 is the annulus area at the rotor exit. The measured static pressure at the rotor exit was taken as the mean of the averaged inner and averaged outer wall-tap values. The stagnation temperature T_3' was taken equal to T_4'. This method of computing the exit stagnation pressure yields a low value because any energy available from the tangential component of the velocity is neglected. Hence, the value of η_t so determined is conservative.

All turbine performance-data were reduced to NACA sea-level standard conditions at the turbine entrance. The performance was expressed in terms of the following parameters:

(1) Brake internal efficiency, η_t

(2) Stagnation pressure ratio, p_1'/p_3'

(3) Equivalent turbine shaft work, E/θ_1

(4) Ratio of blade speed to design blade speed, U/U_{des}

(5) Equivalent weight-flow parameter, $\left(\dfrac{U_m}{\sqrt{\theta_1}}\right)\left(\dfrac{w\sqrt{\theta_1}}{\delta_1}\right)$

The coefficient of aerodynamic loading, as defined in reference 1, is

$$\psi = \frac{2\sin\beta_3 \sin(\beta_2 - \beta_3)}{\sin\beta_2}\frac{1}{\sigma}$$

RESULTS AND DISCUSSION

Over-all performance of the 44-blade-rotor turbine is presented in figure 4(a) in the form of a composite map of turbine parameters. On this map equivalent turbine shaft work is plotted with the equivalent weight-flow parameter; the ratio of blade speed to design blade speed and stagnation pressure ratio are shown as parameters together with contours of brake internal efficiency.

On the performance-map the design point, corresponding to an equivalent work output of 16.14 Btu per pound and equivalent mean blade speed of 625 feet per second, is indicated by a circle. The value of the brake internal efficiency at the design point is 0.89. The stagnation pressure ratio at the design point is 1.74, which is lower than the design value of 1.751 because of the fact that the brake internal efficiency was higher than the design value. The experimental value of the equivalent weight flow was 17.2 pounds per second, which was 3.6 percent higher than the design value.

In figures 4(b), 4(c), and 4(d) are presented the performance maps for the 64-, 32-, and 24-blade-rotor turbines, respectively. On the performance plot for each configuration the design point, indicated by a circle, corresponds to design work output and design equivalent mean

blade speed. For the 64- and 32-blade-rotor turbines, it can be noted that the design point lies close to the region of maximum brake internal efficiency. For the 24-blade-rotor turbine (fig. 4(d)) the maximum stagnation pressure ratio investigated was less than the design value. A choking condition in the annulus downstream of the turbine rotor limited the maximum stagnation pressure ratio attainable experimentally. The general trend of the efficiency contours is the same for each of the four blading solidities. The values of brake internal efficiency at the design points can be seen from this figure to vary with solidity. Figure 4(a) shows that the 44-blade-rotor turbine yielded the highest value of brake internal efficiency at the design point.

The performance parameters at the design points are summarized as follows:

Number of blades	σ	$\dfrac{w\sqrt{\theta_1}}{\delta_1}$	η_t	$\dfrac{p_1{'}}{p_3{'}}$
64	2.27	15.7	0.87	1.79
44	1.56	17.2	.89	1.74
32	1.14	18.0	.89	1.76
24	.85	19.5	.86	----

The maximum brake internal efficiencies obtainable for each stagnation pressure ratio investigated are compared for the four turbine solidities in figure 5. This figure shows that the 44-blade-rotor configuration has a higher value of maximum brake internal efficiency than the other configurations over most of the range of stagnation pressure ratios investigated. The maximum brake internal efficiency obtainable is 0.895 and it occurs at a stagnation pressure ratio of 1.81. Above stagnation pressure ratios of about 1.7, the curve for the 64-blade rotor differs from the other three in that the rate at which maximum brake internal efficiency falls off is much less.

In figure 6(a) is shown the variation of maximum brake internal efficiency with solidity at a stagnation pressure ratio of 1.78, the approximate average design stagnation pressure ratio of the four configurations. This plot shows that for solidities from about 1.1 up to 2.0, for this turbine, a relatively flat curve of maximum brake internal efficiency is realized. The optimum solidity for this turbine is approximately 1.5. These data also show that the variation in the maximum obtainable brake internal efficiency at this stagnation pressure ratio was about 0.03 over the range of solidities investigated. A 45-percent reduction in the number of rotor blades, from 44 to 24, resulted in a 0.03 drop in maximum brake internal efficiency; a 45-percent increase in the number of rotor blades, from 44 to 64, resulted in a 0.02 drop in maximum brake internal efficiency.

The method for determining optimum solidity presented in reference 1 is based on two-dimensional incompressible flow applied to rows of blades in a two-dimensional cascade. This reference concludes that the coefficient of lift referred to the mean velocity of the gas flow through a cascade is unsuitable as a criterion for calculating the optimum solidity because of the large variation of this coefficient with the exit gas angle from the blade row. Introduced in this reference is a "coefficient of aerodynamic loading", which is a coefficient of lift expressed as the ratio of the tangential component of the lift to the exit dynamic head. An optimum value of 0.80 for this coefficient is suggested in this reference. Experimental cascade data have indicated that this value is nearly constant over a wide range of air inlet and exit angles. The method of reference 1 was applied to determine the optimum solidity of the 44-blade-rotor configuration by using the design angles at the mean section. The resulting value of optimum solidity was 1.30, which falls upon the relatively flat portion of the curve (fig. 6(a)).

The desirability of operating at optimum values of lift-drag ratio is explained in reference 2. The coefficient of lift expressed as a ratio of lift to the exit dynamic head is related to solidity for optimum performance. The optimum solidity determined by this method with the aid of the mean design angles of the 44-blade-rotor configuration was 0.91; this value is plotted on the curve of figure 6(a).

The criterion for optimum solidity in reference 3 is minimum blade profile loss. Profile-loss coefficients obtained from two-dimensional cascade studies of nozzle-type blades and impulse blades for varying solidity are presented. In this reference, nozzle-type blades are defined as blades set with zero inlet-blade angle; impulse blades are defined as those such that the inlet-blade angle is equal to the exit-air angle. For blades intermediate between nozzle-type and impulse, empirical rules are given for approximating the profile-loss coefficient. The report indicates that the optimum solidity based on these results differs considerably from the optimum values presented in references 1 and 2 over a wide range of blade angle. An optimum value of solidity was determined by the method of reference 3, again by the use of the mean design angles of the 44-blade-rotor configuration. An optimum mean solidity of 0.96 was determined by this method, and the value is plotted on the curve in figure 6(a). Thus, the methods of references 2 and 3 yield approximately the same value of optimum solidity for this design. This value corresponds to an experimental efficiency of about 0.02 less than that associated with the optimum value of solidity calculated by the method of reference 1.

In figure 6(b) maximum brake internal efficiency is plotted against the coefficient of aerodynamic loading ψ introduced in reference 1. This figure indicates that considerable leeway may be possible in the choice of an optimum value for the coefficient of aerodynamic loading; values of this coefficient from about 0.55 to 1.00 result in calculated

2497

values of solidity associated with the flat, high-efficiency portion of the curve. A value of 0.75 is shown by this figure to be optimum for the turbine of the present investigation.

SUMMARY OF RESULTS

The over-all performance of a conservatively designed turbine suitable for the last stage of a multistage turbine was determined. The turbine was investigated at four rotor solidities in order to determine the effect of solidity upon the over-all performance. The rotor-blade configurations consisted of 64, 44, 32, and 24 blades; the blades of all four configurations were identical. The following are the results obtained:

1. The 44-blade-rotor turbine yielded the highest efficiency over most of the range of investigation. The value of the maximum brake internal efficiency was 0.895. The efficiency at the design point was 0.89.

2. A relatively flat curve of maximum brake internal efficiency was found over most of the range of solidities investigated. A value of solidity of approximately 1.5 was found to be optimum for this turbine. A 45-percent reduction in the number of rotor blades, from 44 to 24, resulted in a decrease in maximum brake internal efficiency of 0.03. A 45-percent increase in the number of rotor blades, from 44 to 64, resulted in a decrease in maximum brake internal efficiency of 0.02.

3. A value for the coefficient of aerodynamic loading of approximately 0.75 was found to be optimum for this turbine. Values of the coefficient of aerodynamic loading from 0.55 to 1.00 resulted in less than a 0.01 drop from the maximum efficiency obtainable experimentally.
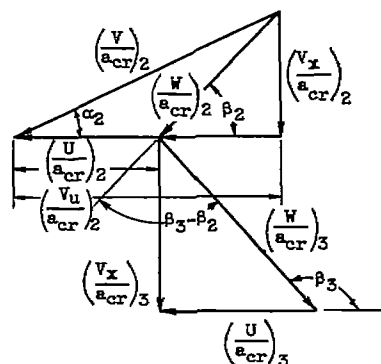
Lewis Flight Propulsion Laboratory
    National Advisory Committee for Aeronautics
        Cleveland, Ohio

REFERENCES

1. Zweifel, O.: Optimum Blade Pitch for Turbo-Machines with Special Reference to Blades of Great Curvature. The Eng. Digest, vol. 7, no. 11, Nov. 1946, pp. 358-360; cont., vol. 7, no. 12, Dec. 1946, pp. 381-383.

2. Howell, A. R., and Carter, A. D. S.: Fluid Flow Through Cascades of
     Aerofoils. Rep. No. R.6, British N.G.T.E., Sept. 1946.

3. Ainley, D. G., and Mathieson, G. C. R.: An Examination of the Flow
     and Pressure Losses in Blade Rows of Axial Flow Turbines. Rep.
     No. R.86, British N.G.T.E., March 1951.

4. Anon.: Fluid Meters, Their Theory and Application. A.S.M.E. Res.
     Pub. by Am. Soc. Mech. Eng. (New York), 4th ed., 1937.

2497

2497

TABLE I - DESIGN VELOCITY COMPONENTS AND FLOW ANGLES FOR 64-, 44-,

32-, AND 24-BLADE-ROTOR CONFIGURATIONS

	Velocity diagram components	Number of rotor blades					
		64	44			32	24
		Section					
		Mean	Hub	Mean	Tip	Mean	Mean
S T A T O R	$\left(\dfrac{U}{a_{cr}}\right)_2$	0.614	0.461	0.614	0.768	0.614	0.614
	$\left(\dfrac{V_u}{a_{cr}}\right)_2$	.656	.846	.634	.508	.649	.655
	$\left(\dfrac{V}{a_{cr}}\right)_2$	.760	.939	.754	.650	.782	.803
	$\left(\dfrac{V_x}{a_{cr}}\right)_2$	.384	.407	.407	.407	.435	.465
	$\left(\dfrac{W}{a_{cr}}\right)_2$	.366	.561	.407	.482	.437	.466
	$\left(\dfrac{W''}{a_{cr}}\right)_2$	.401	.589	.422	.490	.453	.484
	α_2	30.4°	25.7°	32.7°	38.7°	33.9°	35.4°
	β_2	83.7°	46.5°	87.2°	122.5°	85.4°	85.0°
R O T O R	$\left(\dfrac{U}{a_{cr}}\right)_3$	0.660	0.493	0.658	0.822	0.659	0.660
	$\left(\dfrac{V_u}{a_{cr}}\right)_3$	0	0	0	0	0	0
	$\left(\dfrac{V}{a_{cr}}\right)_3$	.556	.590	.590	.590	.646	.708
	$\left(\dfrac{V_x}{a_{cr}}\right)_3$	.556	.590	.590	.590	.646	.708
	$\left(\dfrac{W}{a_{cr}}\right)_3$	.862	.769	.884	1.012	.923	.968
	$\left(\dfrac{W''}{a_{cr}}\right)_3$	.833	.754	.854	.960	.892	.935
	α_3	90.0°	90.0°	90.0°	90.0°	90.0°	90.0°
	β_3	139.9°	129.9°	138.1°	144.3°	135.6°	133.0°
	$\beta_3-\beta_2$	56.1°	83.4°	51.0°	21.8°	50.1°	48.0°
	F_h	0.50	0.64			0.62	0.67

Air flow

Axial direction

Hub-section radius, 4.20 in.

25.3°

Trailing-edge radius, 0.010 in.

Leading-edge radius, 0.025 in.

32.9°

Mean-section radius, 5.60 in.

38.7°

Tip-section radius, 7.00 in.

x (in.)	y	
	Suction, in.	Pressure, in.
0	0.050	0.050
.1	.026	.115
.2	.046	.160
.4	.122	.261
.6	.243	.392
.8	.418	.555
1.0	.683	.773
1.2	1.076	1.123
1.25	1.185	1.183

x (in.)	y	
	Suction, in.	Pressure, in.
0	0.050	0.050
.1	.026	.108
.2	.044	.150
.4	.106	.247
.6	.214	.365
.8	.382	.508
1.0	.630	.697
1.2	.939	.977
1.25	1.020	1.020

x (in.)	y	
	Suction, in.	Pressure, in.
0	0.050	0.050
.1	.023	.104
.2	.040	.141
.4	.103	.230
.6	.214	.340
.8	.381	.482
1.0	.614	.663
1.2	.863	.897
1.25	.930	.930

(a) Stator blade.

Figure 1. - Blade-section profiles and coordinates for 44-blade-rotor-turbine configuration.

Hub-section radius, 4.20 in.

x (in.)	y	
	Suction, in.	Pressure, in.
0	0.735	0.735
.1	.616	.725
.2	.549	.687
.3	.512	.661
.5	.489	.637
.7	.516	.654
.9	.594	.701
1.10	.728	.789
1.25	.851	.851

Mean-section radius, 5.60 in.

x (in.)	y	
	Suction, in.	Pressure, in.
0	0.397	0.397
.1	.362	.451
.2	.359	.486
.3	.372	.521
.5	.448	.598
.7	.548	.690
.9	.702	.808
1.1	.902	.961
1.25	1.063	1.063

Tip-section radius, 7.00 in.

x (in.)	y	
	Suction, in.	Pressure, in.
0	0.105	0.105
.1	.114	.215
.2	.164	.298
.3	.230	.377
.5	.388	.541
.7	.574	.713
.9	.801	.900
1.1	1.056	1.110
1.25	1.253	1.253
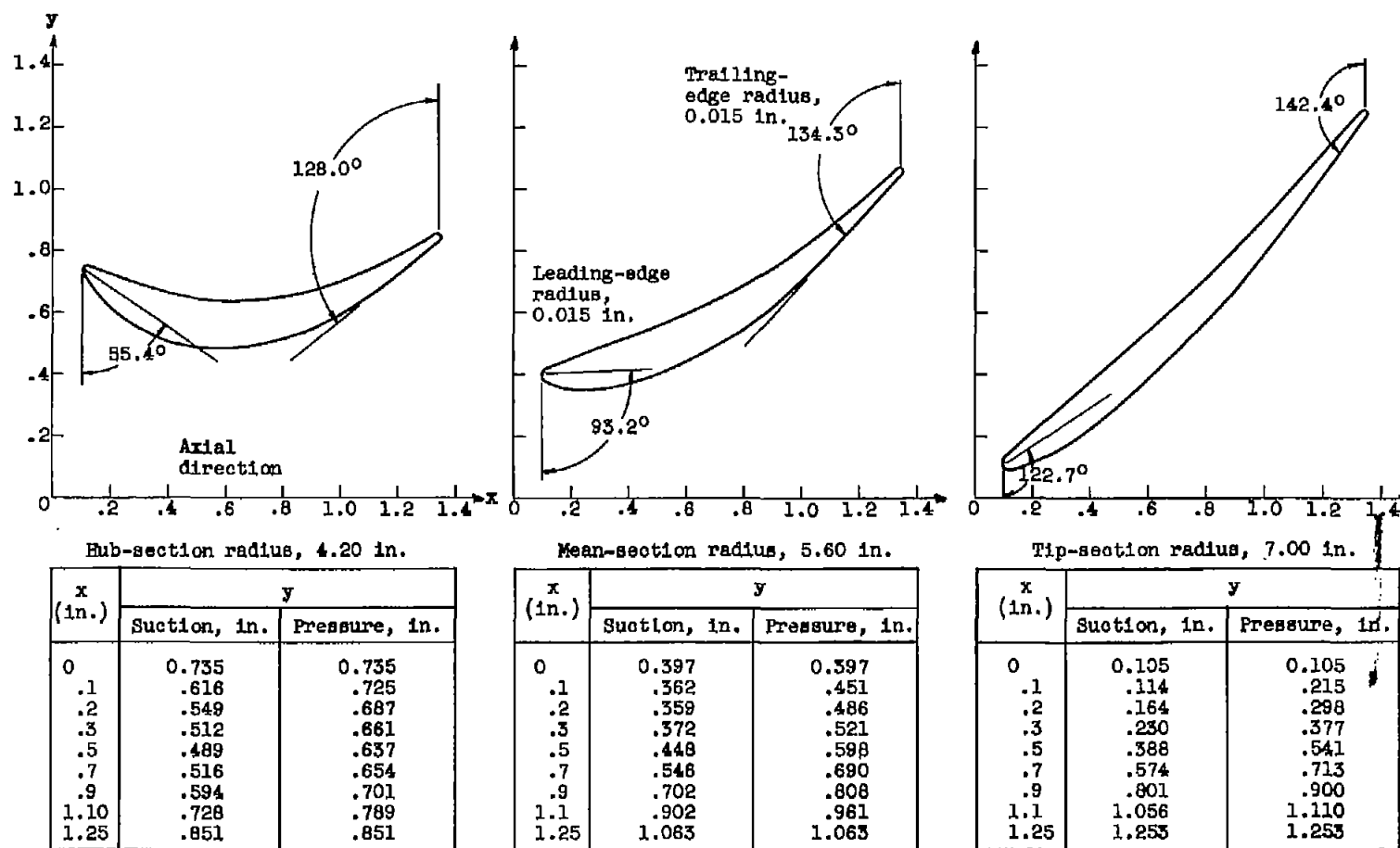
(b) Rotor blade.

Figure 1. - Concluded. Blade-section profiles and coordinates for 44-blade-rotor-turbine configuration.
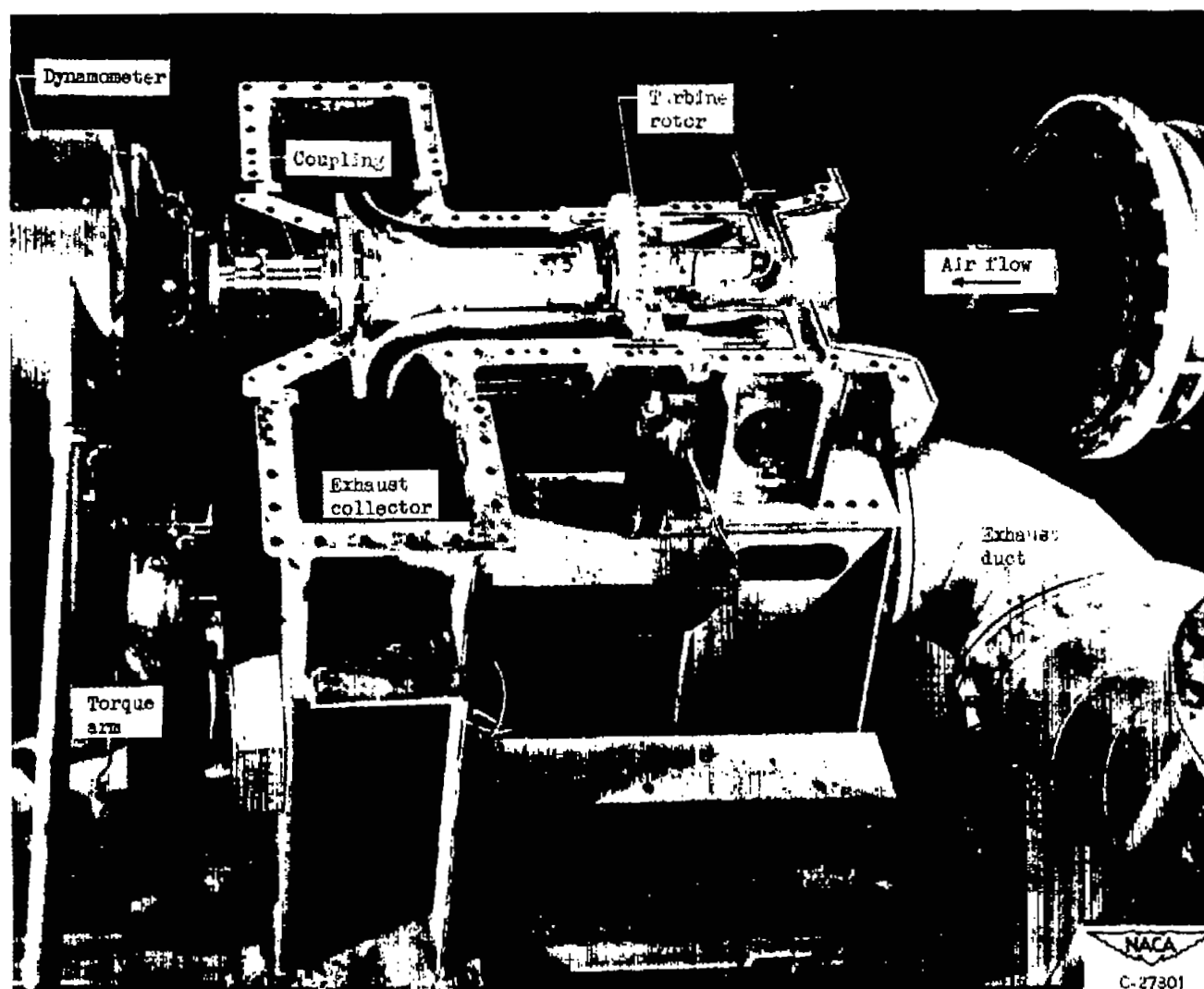
Figure 2. - Turbine installation with top half of casing removed.
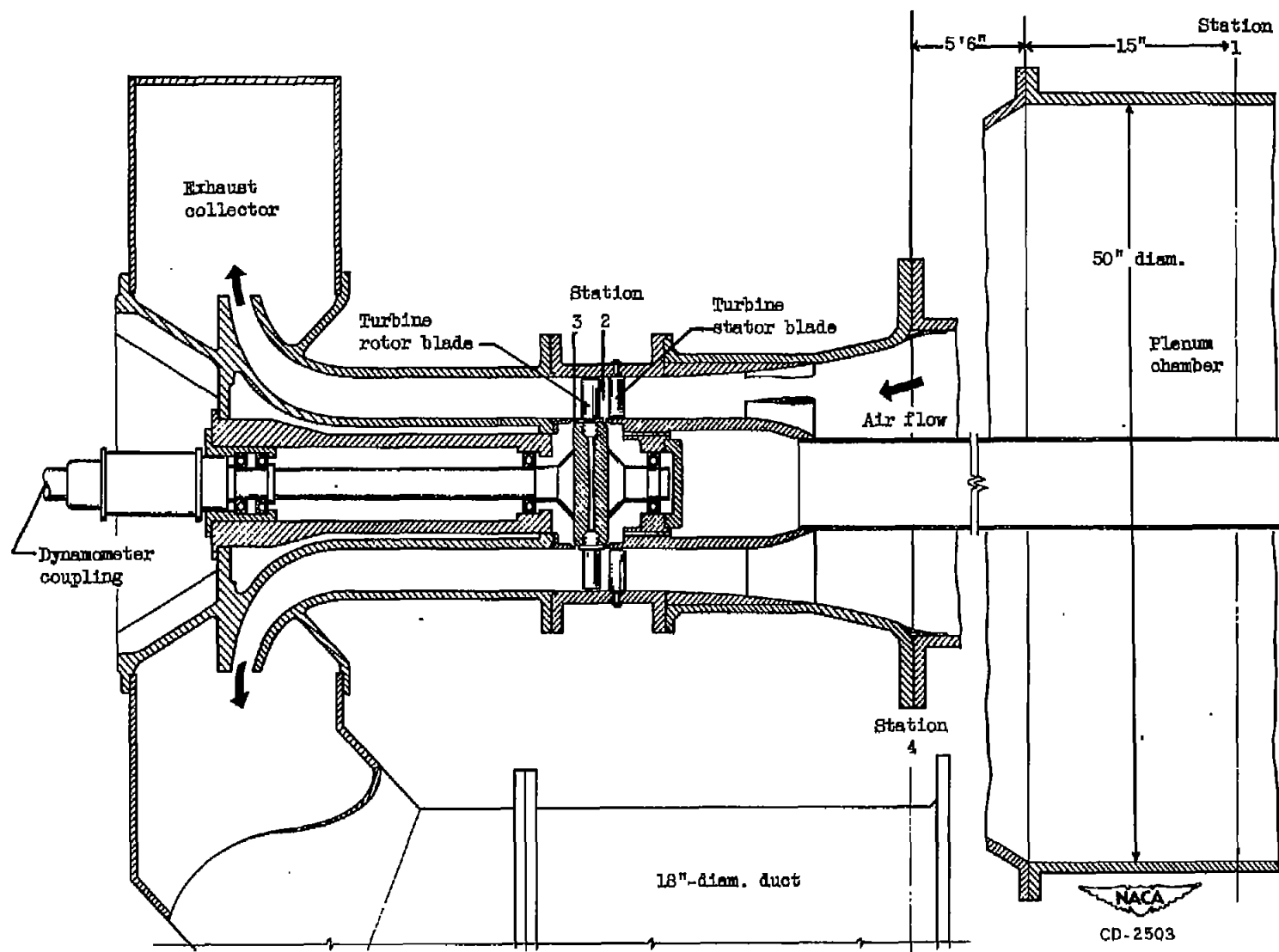
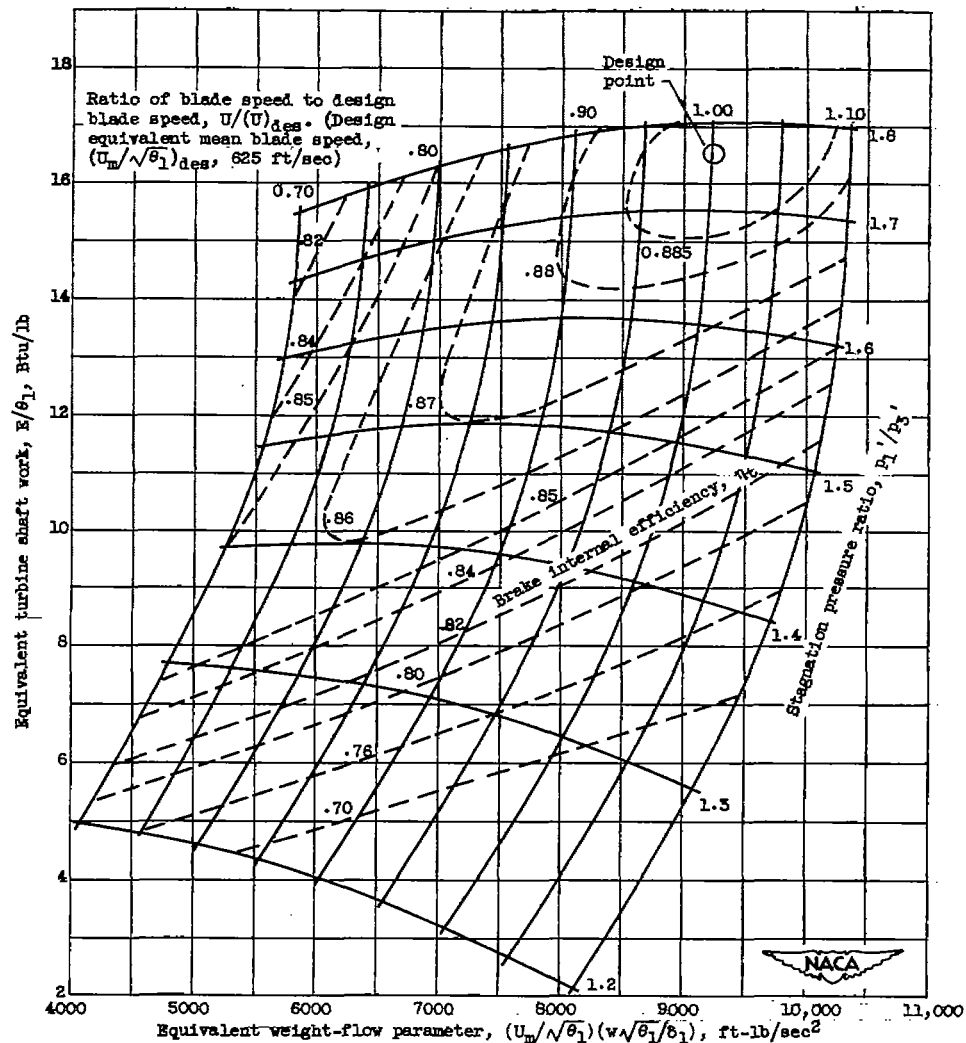Figure 3. - Schematic section of turbine installation showing measuring stations.
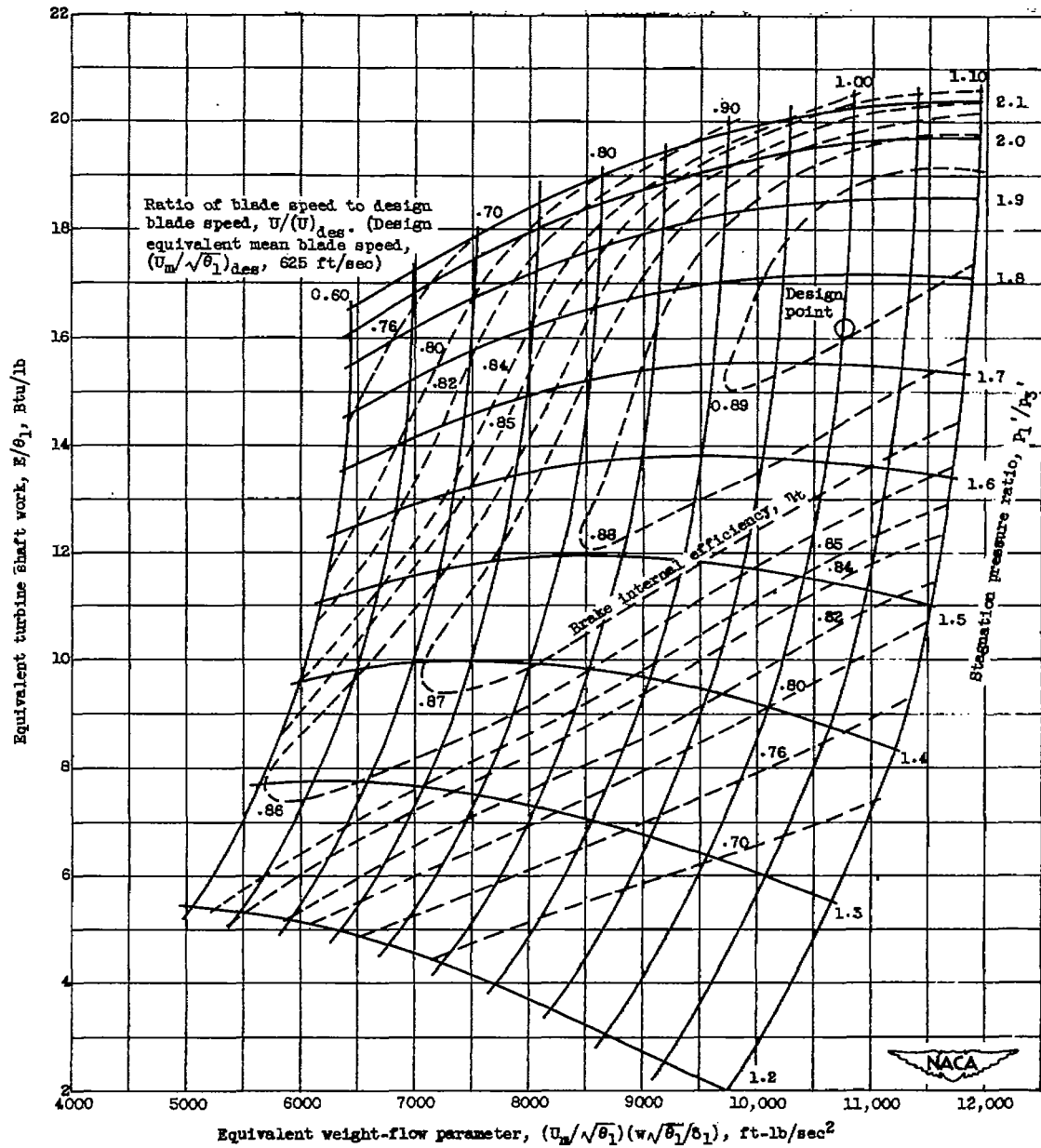
(a) 44-blade-rotor-turbine configuration.

Figure 4. - Over-all turbine performance.
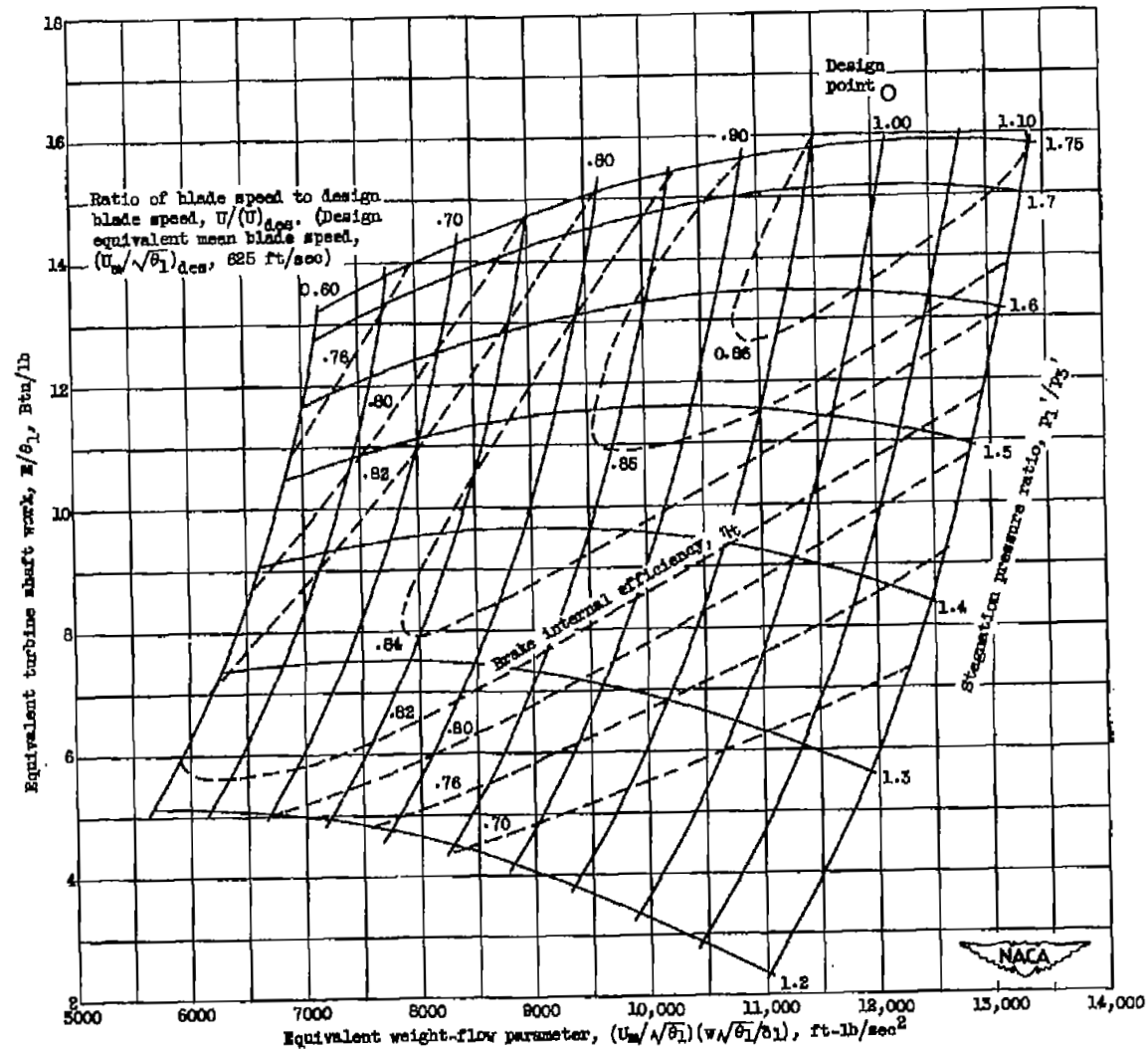
2497
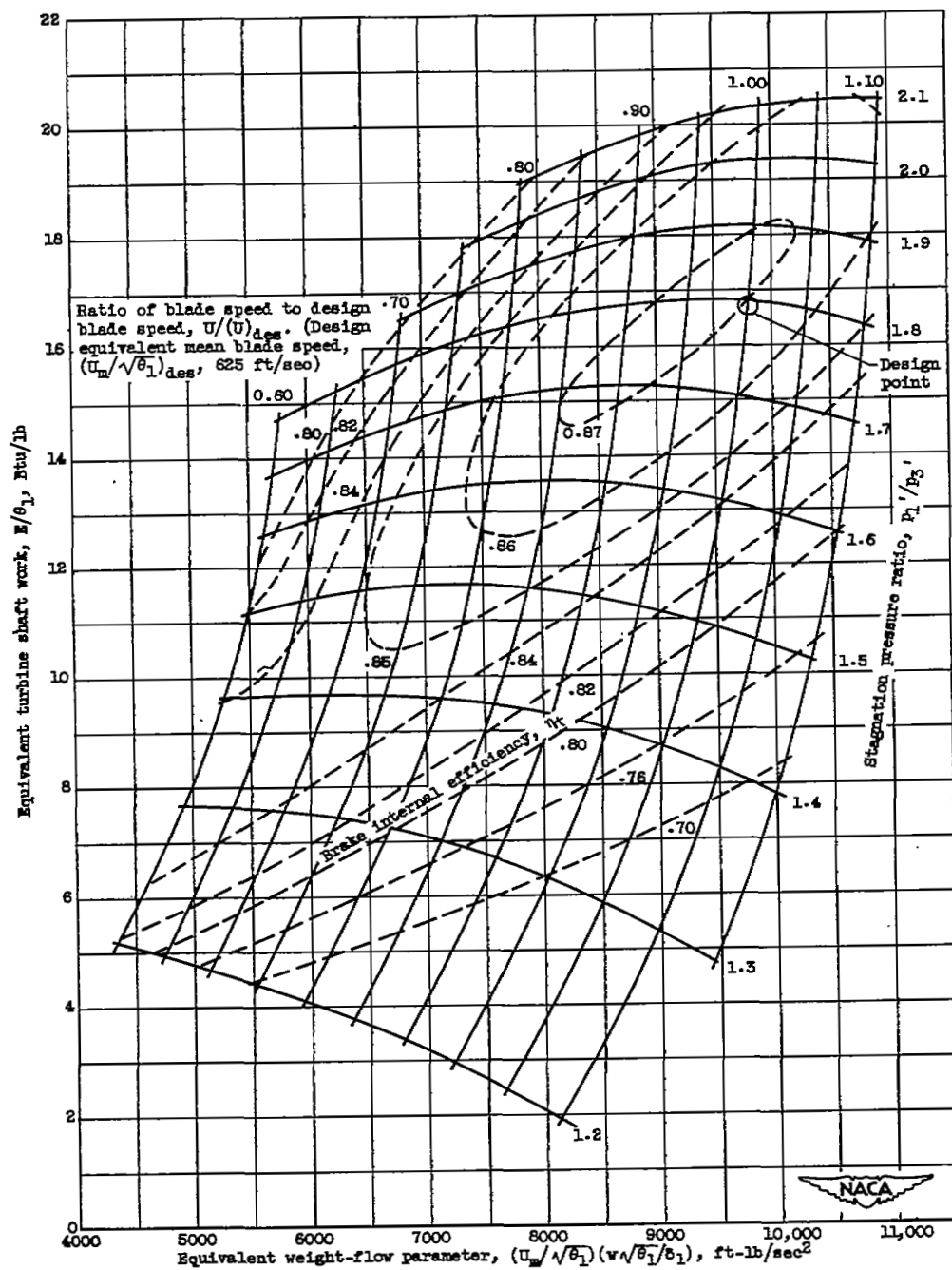
(b) 64-blade-rotor-turbine configuration.

Figure 4. - Continued. Over-all turbine performance.

(c) 32-blade-rotor-turbine configuration.

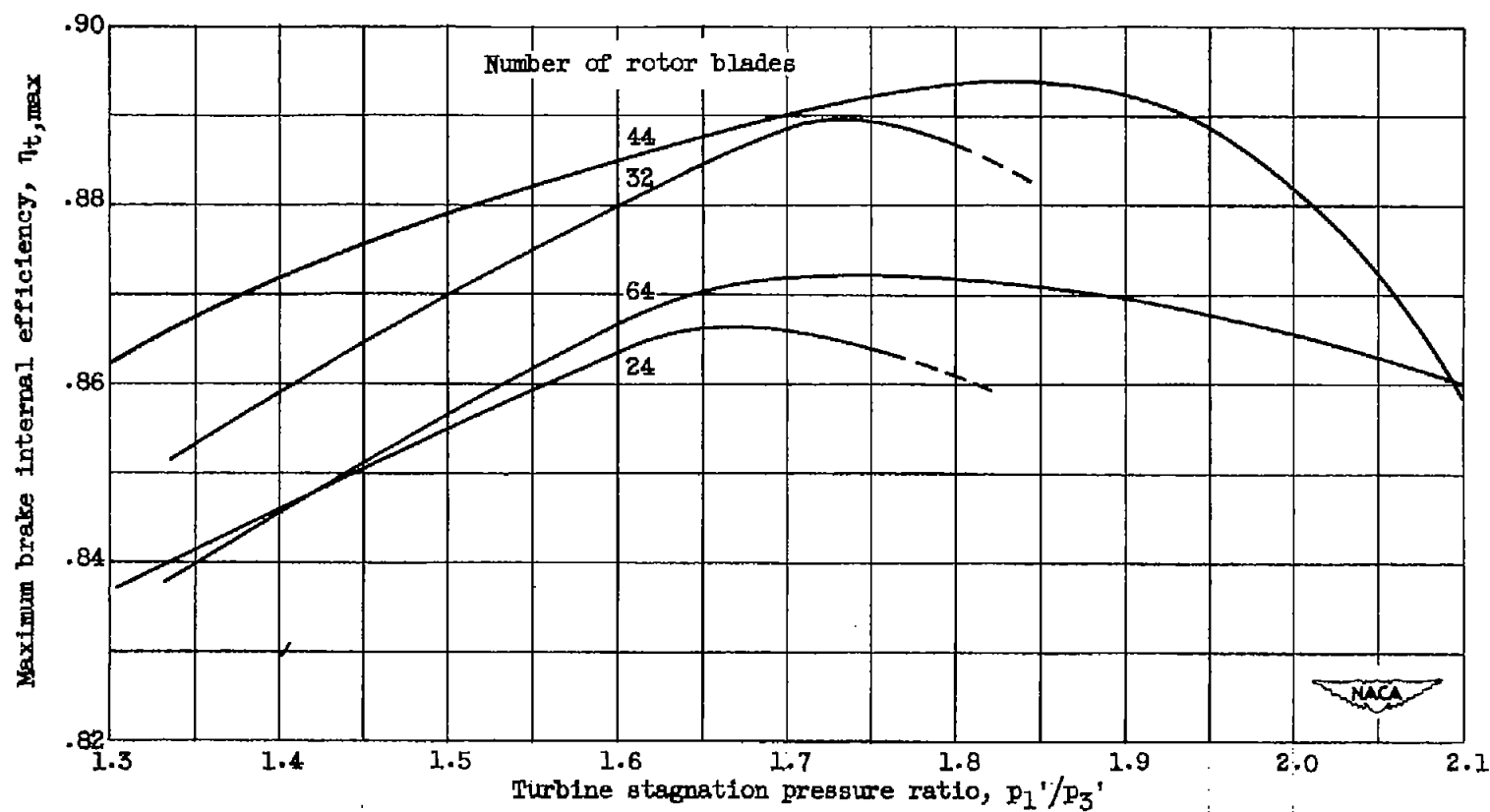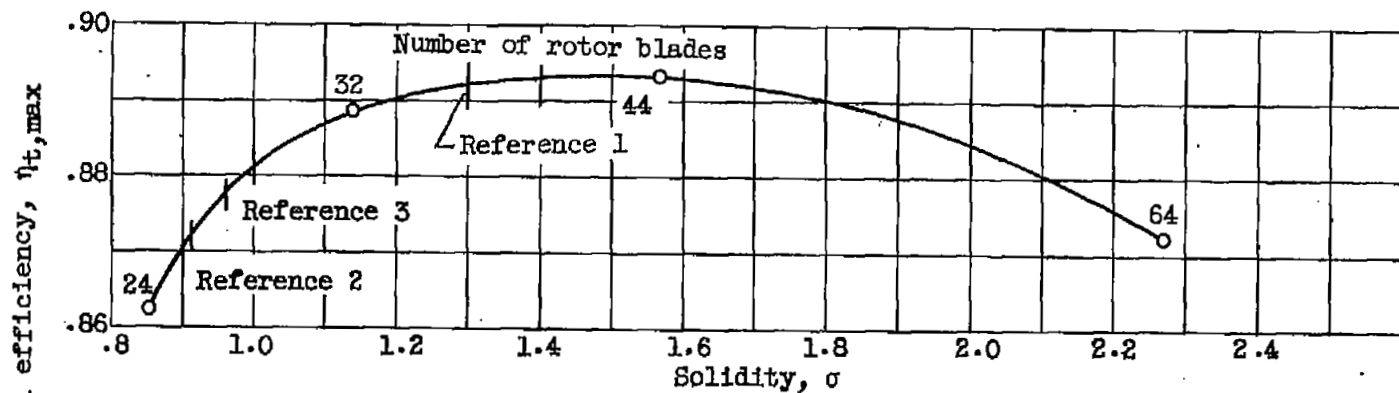Figure 4. - Continued. Over-all turbine performance.

(d) 24-blade-rotor-turbine configuration.
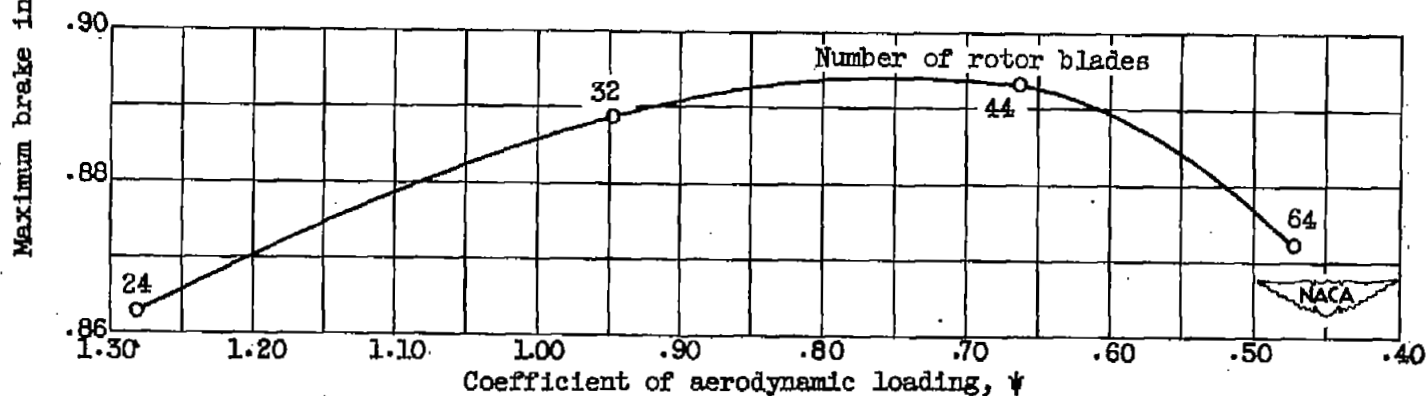
Figure 4. - Concluded. Over-all turbine performance.

Figure 5. - Maximum brake internal efficiency obtainable at each stagnation pressure ratio.
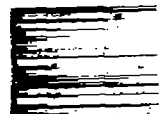
(a) Variation with solidity.

(b) Variation with coefficient of aerodynamic loading.

Figure 6. - Maximum brake internal efficiency obtainable at 1.78 stagnation pressure ratio.